Influence of the Lamellar Phase Unbinding Energy on the Relative Stability of Lamellar and Inverted Cubic Phases

D. P. Siegel* and B. G. Tenchov†
*Givaudan Inc., Cincinnati, Ohio 45216; and †Northwestern University, Department of Biochemistry, Molecular Biology and Cell Biology, Evanston, Illinois 60208

ABSTRACT Based on curvature energy considerations, nonbilayer phase-forming phospholipids in excess water should form stable bicontinuous inverted cubic (Q_{II}) phases at temperatures between the lamellar (L_α) and inverted hexagonal (H_{II}) phase regions. However, the phosphatidylethanolamines (PEs), which are a common class of biomembrane phospholipids, typically display direct L_α/H_{II} phase transitions and may form intermediate Q_{II} phases only after the temperature is cycled repeatedly across the L_α/H_{II} phase transition temperature, T_H, or when the H_{II} phases are cooled from $T > T_H$. This raises the question of whether models of inverted phase stability, which are based on curvature energy alone, accurately predict the relative free energy of these phases. Here we demonstrate the important role of a noncurvature energy contribution, the unbinding energy of the L_α phase bilayers, g_u, that serves to stabilize the L_α phase relative to the nonlamellar phases. The planar L_α phase bilayers must separate for a Q_{II} phase to form and it turns out that the work of their unbinding can be larger than the curvature energy reduction on formation of Q_{II} phase from L_α at temperatures near the L_α/Q_{II} transition temperature (T_Q). Using g_u and elastic constant values typical of unsaturated PEs, we show that g_u is sufficient to make $T_Q > T_H$ for the latter lipids. Such systems would display direct $L_\alpha \rightarrow H_{II}$ transitions, and a Q_{II} phase might only form as a metastable phase upon cooling of the H_{II} phase. The g_u values for methylated PEs and PE/phosphatidylcholine mixtures are significantly smaller than those for PEs and increase T_Q by only a few degrees, consistent with observations of these systems. This influence of g_u also rationalizes the effect of some aqueous solutes to increase the rate of Q_{II} formation during temperature cycling of lipid dispersions. Finally, the results are relevant to protocols for determining the Gaussian curvature modulus, which substantially affects the energy of intermediates in membrane fusion and fission. Recently, two such methods were proposed based on measuring T_Q and on measuring Q_{II} phase unit cell dimensions, respectively. In view of the effect of g_u on T_Q that we describe here, the latter method, which does not depend on the value of g_u, is preferable.

INTRODUCTION

Although their basic building elements are liquid crystalline lipid bilayers, biomembranes also contain a large fraction of lipids able to form inverted nonlamellar phases under physiological conditions (1,2). For example, the phosphatidylethanolamines (PEs), which are a common, widely spread membrane lipid class, easily transform from lamellar, L_α, into inverted hexagonal, H_{II}, or, occasionally, into inverted bicontinuous cubic, Q_{II}, phase in aqueous dispersions (3). Many glycolipids can also form nonlamellar phases (4). Under specific conditions, such as low pH or the presence of divalent cations, inverted nonlamellar phases can also be induced in phosphatidylserines, cardiolipins, and phosphatidic acids. Moreover, it has been shown recently that total and polar lipid extracts and membrane-mimicking lipid compositions also readily form nonlamellar phases at close to physiological temperatures (5). Several different types of inverted nonlamellar phases have been found to form in fully hydrated dispersions of membrane lipids, all of them appearing at temperatures above the existence range of the lamellar liquid crystalline phase L_α. In a hypothetical ''full'' phase sequence, these phases arrange in the following order with increase of temperature:

$$L_\alpha \rightarrow Q_{II} \rightarrow H_{II} \rightarrow Q_{II}^{M} \rightarrow M_{II}.$$

L, Q, H, and M refer to lamellar, cubic, hexagonal, and micellar phases, respectively. Q_{II} denotes a set of three inverted bicontinuous (bilayer) cubic phases, Im3m, Pn3m, and Ia3d, each of which may appear depending on lipid type and specific conditions.

In this work we address a problem related to the relative stabilities of the L_α and Q_{II} phases. It is known from a number of studies that dispersions of double-chain nonlamellar membrane lipids most frequently display a direct lamellar-inverted hexagonal, $L_\alpha \rightarrow H_{II}$, phase transition, omitting the intermediate Q_{II} phase. The $L_\alpha \rightarrow Q_{II}$ transitions, followed by H_{II} formation at higher temperature, are relatively rare, and they are typically observed for short-chain PEs and glycolipids (6,7). Similarly, mixtures of saturated phosphatidylcholines (PCs) and fatty acids with shorter lauric and myristic acyl chains can form intermediate Q_{II} phase, whereas mixtures with longer chains (palmitic, stearic) again display direct $L_\alpha \rightarrow H_{II}$ transitions (8). However, it was shown for several PEs, which display direct $L_\alpha \rightarrow H_{II}$ phase transitions, that they can be converted into the intermediate Q_{II} phase when the temperature is cycled repeatedly across

Submitted July 24, 2007, and accepted for publication January 3, 2008.

Address reprint requests to D. P. Siegel, E-mail: david.siegel@givaudan.com.

Editor: Thomas J. McIntosh.

0006-3495/08/05/3987/09 $2.00

doi: 10.1529/biophysj.107.118034

the L_α/H_{II} phase transition (9–13). In these cases, traces of Q_{II} phase were found to form on cooling from the H_{II} range and to gradually replace the initial lamellar L_α phase over the whole range of its existence (11). These observations suggest that the bilayer Q_{II} phases are metastable with respect to L_α in PEs with intermediate chain lengths of 16–18 carbon atoms such as dielaidoyl PE (DEPE), dipalmitoyl PE (DPPE), dihexadecyl PE (DHPE), dipalmitoleoyl PE (DPoPE), and dioleoyl PE (DOPE).

On the other hand, the $L_\alpha \rightarrow Q_{II} \rightarrow H_{II}$ sequence of phases can be obtained theoretically if the free energy differences between these phases are assumed to be due only to differences in their curvature energies (e.g., Siegel and Kozlov (14) and Siegel (15)). Thus the absence of Q_{II} phase on the heating of most PEs, in particular those with intermediate and longer chains, raises the question of to what extent theoretical descriptions of the curvature energies of Q_{II} and H_{II} phases are sufficient to predict the relative stability of these phases, especially the thermodynamic stability of a Q_{II} phase with respect to the neighboring L_α and H_{II} phases.

Here we show that the apparent discrepancy between experimental observations and curvature energy considerations can be resolved by taking into account a noncurvature energy contribution, the unbinding energy, g_u, of the L_α phase, which stabilizes the lamellar phase relative to the Q_{II} and H_{II} phases. The planar L_α phase bilayers must separate for Q_{II} phase to form and it turns out that the work of their unbinding can be larger than the curvature energy reduction upon formation of Q_{II} from the L_α phase. Using g_u values and values of elastic constants typical of unsaturated PEs, we show that g_u is sufficiently large to shift the temperature T_Q of the $L_\alpha \rightarrow Q_{II}$ transition to values above the temperature T_H of the $L_\alpha \rightarrow H_{II}$ transition. Such systems with $T_Q > T_H$ would display direct $L_\alpha \rightarrow H_{II}$ transitions, and a Q_{II} phase might only form as a metastable phase upon cooling from the H_{II} phase region.

These results have important implications for the choice of methods that can be used to determine the Gaussian curvature elasticity modulus. This modulus has a substantial effect on the energy of intermediates in the process of membrane fusion and fission, and the contribution of the Gaussian curvature elastic energy to the energy of fusion intermediates is on the same order of magnitude as the contribution of the bending energy (16).

THEORY

Curvature energy differences between lamellar and nonlamellar phases

If the free energy differences between lamellar and nonlamellar phases are assumed to be due only to curvature energy, one would obtain that a lipid system exhibits an $L_\alpha \rightarrow Q_{II} \rightarrow H_{II}$ sequence of phases with increasing temperature (14,15). This is because the spontaneous curvature of lipid monolayers, J_s, becomes more negative with increasing temperature. Respectively, the L_α phase should give way to a Q_{II} phase where the monolayers can adopt more negative mean curvatures while adopting slightly unfavorable Gaussian curvature. At still higher T, the H_{II} phase has a more negative mean curvature energy than Q_{II}. In the H_{II} phase, the monolayer curvature becomes $\approx J_s$, although at the penalty of overcoming unfavorable interstice-packing energies at the boundaries between the H_{II} phase cylinders.

As is known, the quadratic terms in the Helfrich phenomenological membrane curvature energy equation are insufficient to explain the bicontinuous Q_{II} phase stability (Discussion). We therefore use here a previously derived expression for the curvature energy per lipid molecule in the Q_{II} phase with respect to planar bilayers, which is accurate to fourth order in curvature (15). Here we delineate its derivation. The model in Siegel (15) is based on the Helfrich model for the curvature energy (17), complemented with the third- and fourth-order curvature terms as formulated by Mitov (18). The curvature energy of the lipid monolayers is then given by

$$f_i = A_i\left[\frac{k_m}{2}(J_i - J_s)^2 + \kappa K_i + \eta_1 J_i^3 + \eta_2 J_i K_i + \eta_3 J_i^4 + \eta_4 J_i^2 K_i + \bar{\bar{\kappa}} K_i^2\right], \quad (1)$$

where the subscripts i are labels for the two monolayers of the bilayer, and A_i is the area of each monolayer; k_m and κ are the bending (splay) modulus and the Gaussian (saddle splay) modulus of the lipid monolayers, respectively; J_i, J_s, and K_i are the mean curvature at the monolayer neutral plane, the spontaneous curvature at the neutral plane, and the Gaussian curvature of the monolayers, respectively; and finally, η_j and $\bar{\bar{\kappa}}$ are the elastic moduli of the respective third- and fourth-order curvature terms.

Assuming a constant displacement δ of the monolayer neutral planes from the bilayer midplanes, and using a mathematical relationship between the curvatures of parallel surfaces (19), J_i, K_i, and A_i of the monolayers can be expressed in terms of mean curvature, Gaussian curvature, and area (J, K, and A, respectively) of the bilayer midplane. Since the bilayer midplanes of bicontinuous Q_{II} phases lie on minimal surfaces, $J = 0$. It is found that the values of J_i and K_i for the two monolayers are equivalent, and

$$J_i = \frac{2\delta K}{(1+\delta^2 K)}; \quad K_i = \frac{K}{(1+\delta^2 K)}; \quad A_i = A(1+\delta^2 K). \quad (2)$$

The curvature energy per unit area of the bilayer can then be expressed in terms of f_i. Expressing $(1 + \delta^2 K)^{-1}$ as a series of powers of $\delta^2 K$ and collecting terms with the same powers of K, the curvature energy per unit area of bilayer to fourth order in curvature (K^2) is

$$f_B = (1+\delta^2 K)(2f_i) = \kappa_1 K + \kappa_2 K^2, \quad (3)$$

where

$$\kappa_1 = 2\kappa - 4\delta k_m J_s + \delta^2 k_m J_s^2, \quad (4)$$

and

$$\kappa_2 = 4\delta^2 k_m + 4\delta\eta_2 + 2\bar{\bar{\kappa}}. \quad (5)$$

The area average of Eq. 3 is the energy per unit area of the bilayer in the Q_{II} phase. The integrals of K^N over the unit cells of the different Q_{II} phases are

$$\int_{\text{unit cell}} K^N dA = \frac{S_N}{c^{(2N-2)}}, \quad (6)$$

where c is the cell constant of the Q_{II} phase and the coefficients S_N are geometric constants that have been calculated numerically for each of the infinite periodic minimal surfaces corresponding to the different Q_{II} phases (20,21). The area-averaged curvature energy is then

$$\langle f_B \rangle = \kappa_1\left(\frac{S_1}{S_0}\right)\left[\frac{1}{c^2}\right] + \kappa_2\left(\frac{S_2}{S_0}\right)\left[\frac{1}{c^4}\right]. \quad (7)$$

We find the equilibrium value of c in excess water, c_{eq}, by minimizing Eq. 7 with respect to c at constant J_s (constant temperature). This yields

$$c_{eq} = \sqrt{-\frac{2\kappa_2 S_2}{\kappa_1 S_1}} = \sqrt{-\left(\frac{\kappa_2}{k_m}\right)\left(\frac{S_2}{S_1}\right)\frac{1}{(M-x)}}, \quad (8)$$

where, in the second equality, we have inserted Eq. 4 and simplified notation by making the substitutions

$$x = 2\delta J_s - \frac{\delta^2 J_s^2}{2}; \quad M = \frac{\kappa}{k_m}. \quad (9)$$

The result of Eq. 8 is a real number because $S_1 < 0$, and κ_1, κ_2, and S_2 are all positive in the range of application of this expression (see below). Substituting Eqs. 8 and 9 into Eq. 7 and dividing by the number of lipid molecules per unit area of bilayer yields the equilibrium curvature energy per lipid molecule in the Q_{II} phase in excess water:

$$\mu_Q^c = -\frac{a}{2}\left(\frac{S_1^2}{S_0 S_2}\right)\frac{k_m (M-x)^2}{(\kappa_2/k_m)}. \quad (10)$$

$S_1^2/S_0 S_2 = 0.820545$ for all three Bonnet-related Q_{II} phases (Im3m, Pn3m, and Ia3d). δ is ~1.3 nm for phospholipids with oleoyl chains, and a is the area per lipid molecule at the neutral surface. The values of M and the ratio κ_2/k_m can be determined experimentally from the temperature dependence of the Q_{II} unit cell constant in excess water using Eqs. 8 and 9 if the values of δ, J_s, and k_m are known over the relevant range of temperature (see below). For *N*-monomethylated dioleoylphosphatidylethanolamine (DOPE-Me), using the data in (22), $M = -0.90 \pm 0.09$ and $\kappa_2/k_m = 2.4 \pm 0.3$ nm^2 (15).

An important feature of the Q_{II} curvature energy model in Eq. 10 is that it predicts the existence of a threshold temperature, T_K, limiting from below the range of Q_{II} stability. J_s decreases with increasing temperature, and T_K is the temperature at which $x = M$ (Eq. 9). Above T_K, the curvature energy is always negative ($\mu_Q^c < 0$), rendering the Q_{II} phase more stable than L_α. At T_K, μ_Q^c becomes equal to 0 and the Q_{II} phase unit cell constant diverges to infinity. No finite equilibrium values for the Q_{II} unit cell constant exist below that temperature (15). T_K is the lowest temperature at which formation of stable structures with negative Gaussian curvature, like Q_{II} phases, is still possible in the given lipid system. The value of T_K is determined by the balance of elastic constants and spontaneous curvature of the lipid membrane, through the temperature dependence of J_s and Eq. 9. For supercooled Q_{II} phases at $T < T_K$, the curvature energy is positive and is not given by Eq. 10. Its value and the nonequilibrium value of the Q_{II} unit cell constant depend on the temperature history of the lipid sample and will not be discussed further here.

The curvature energy per lipid molecule in the H_{II} phase in excess water with respect to planar bilayers is (14)

$$\mu_H^c = \frac{a k_m}{2}\left((J_s(T_H))^2 - (J_s(T))^2\right). \quad (11)$$

Here $J_s(T_H)$ is the value of J_s at the observed L_α/H_{II} transition temperature, T_H.

In the absence of other contributions, the free energy differences between the L_α phase and the Q_{II} and H_{II} phases are given by the curvature energies μ_Q^c and μ_H^c, respectively. In Fig. 1 *A*, μ_Q^c and μ_H^c are plotted as a function of temperature using parameters determined for DOPE-Me (15). The values for k_m and δ are 10 k_BT and 1.3 nm, respectively, and $a = 0.6$ nm^2. The values of $J_s(T)$ are taken from Siegel and Kozlov (14), and the calculated threshold temperature, T_K, is 50°C (15). The observed value of T_H for DOPE-Me is 62°C (22). The curvature energy plots in Fig. 1 *A* should be representative also for DOPE and mixtures of DOPE with 5–30 mol % DOPC at temperatures near the respective T_H, because of similar H_{II} phase lattice constants as a function of temperature (23,24) and similar values of k_m for DOPE and DOPC (25). This means that J_s in the temperature range of the bilayer/nonbilayer phase transitions and k_m of these lipids should be similar to those of DOPE-Me. The same can also be said for PEs with effective chain lengths of 18 carbons and a variety of acyl chain structures including *cis*- and *trans*-

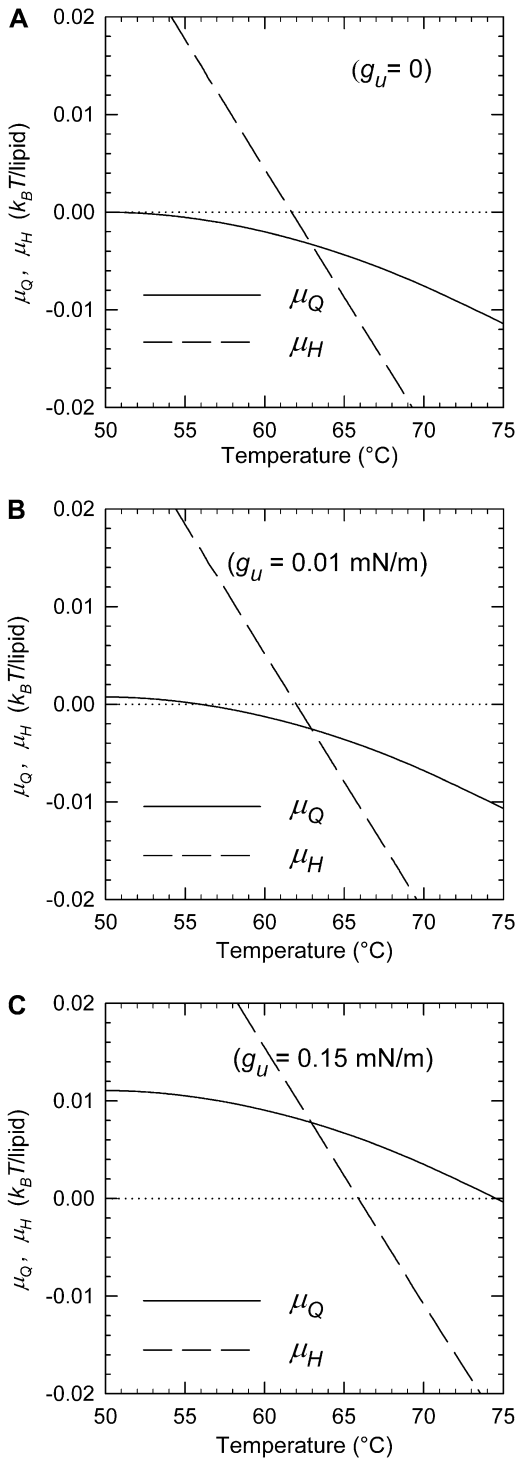

FIGURE 1 Free energy per lipid molecule of the Q_{II} (μ_Q) and H_{II} (μ_H) phases relative to the L_α phase as functions of the temperature for a lipid with the curvature energy parameters of DOPE-Me for different values of the L_α phase unbinding energy, g_u. (*A*) $g_u = 0$ (i.e., μ_Q and μ_H are determined only by curvature elastic energy via Eqs. 10 and 11, respectively). (*B*) $g_u = 0.01$ erg/cm^2, a value typical of methylated PEs and mixtures of PEs with small mole fractions of PC (Table 1). (*C*) $g_u = 0.15$ erg/cm^2, a value typical of pure PEs (Table 1). The curvature elastic energy parameters for DOPE-Me are from Siegel and Kozlov (14) and Siegel (15).

monounsaturated chains and saturated chains with methyl, dimethyl, ethyl, or cylcohexyl substitution near the methyl terminals (23,26–28). Based on curvature energy considerations alone, lipids with these values of the elastic constants should form stable Q_{II} phases in a temperature range below T_H, except for lipids with a value of κ/k_m that is very close to -1 (14,15). However, the few measurements of κ to date indicate that κ is significantly less negative (closer to zero) than this (14,15,29).

Unbinding energy of lamellar phases

Bilayers in lamellar phases interact across the interlamellar water spaces by a combination of attractive and repulsive forces (van der Waals, hydration, and electrostatic and bilayer undulation forces; see Nagle and Tristram-Nagle (30) for a recent review). In addition, PE bilayers may bind to each other by formation of hydrogen bonds between phospholipid headgroups in adjacent interfaces at separations of <1 nm (31). The interplay of these forces generates an interbilayer potential typically with a minimum at a given interbilayer distance (water layer thickness). For lamellar phases in excess water, the bilayers adopt the interbilayer separation corresponding to this minimum. The unbinding energy, g_u, is the work per unit area required to separate these bilayers to infinite separation from the equilibrium interbilayer separation. In separating the bilayers, most of g_u is expended in increasing the interbilayer separation by the first several nanometers.

The unbinding energy can be evaluated through analysis of x-ray diffraction experiments on osmotically stressed multilamellar liposomes (32) or determined more directly by optically measuring the deformation of adhering giant unilamellar vesicles as a function of membrane tension applied by pipette aspiration (33,34). Values of the unbinding energy for a number of lipid systems are summarized in Table 1 (32,35,36).

Contributions of the unbinding energy to the free energies of the Q_{II} and H_{II} phases relative to the L_α phase

The bilayers in a lamellar phase must separate by several nanometers to form a bicontinuous Q_{II} phase. This is necessary because the typical distances between lipid/water interfaces in bicontinuous Q_{II} phases, which are composed of labyrinths of bilayers, are significantly greater than those in the L_α phase. The average separation is given by twice the average water channel radius, r_w (37):

$$r_w = Bc_{eq} - l, \tag{12}$$

where B is a geometric constant specific to the space group of each Q_{II} phase, and l is the lipid monolayer thickness, typically ~2 nm. B is 0.305 for the Im3m, 0.391 for the Pn3m, and 0.248 for the Ia3d cubic phases. Since the Q_{II} unit cell constants for PEs can be >20–25 nm (11), the average bilayer separations in these Q_{II} phases exceed 10–15 nm and are far larger than the typical L_α interlamellar separations of ~2 nm or less.

TABLE 1 Unbinding energies of the lamellar L_α phase of lipid systems

Lipid system	g_u (erg/cm^2)	Reference
POPE	>0.15	(36)
POPE (30°C)	0.14	(32)
Egg-PE	0.14	(32)
N-monomethylated egg-PE	0.01	(32)
POPE/SOPC = 9/1	0.06	(36)
POPE/SOPC = 4/1	0.04	(36)
DOPE/DOPC = 3/1	0.03	(32)
SOPC, egg-PC, and DMPC	0.01–0.015	(34)
Egg-PC/cholesterol = 1/1	0.003	(32)

Unless otherwise noted, the measurement temperature was 22°C.

Since the only attractive interaction at bilayer separations above 1 nm is the van der Waals interaction, the bilayer interaction energy in a Q_{II} phase can be approximated with the van der Waals term for flat bilayers at the average interbilayer separation. The van der Waals energy of two parallel bilayers is given by (30)

$$g_{vdW} = -\frac{A_H}{12\pi}\left[\frac{1}{d^2} - \frac{2}{(d+h)^2} + \frac{1}{(d+2h)^2}\right], \tag{13}$$

where A_H is the Hamaker constant, d is the distance between the bilayers, and h is the bilayer thickness. The distance dependence of g_{vdW} is more complicated in Q_{II} phases because the bilayers are bent into complex shapes and it is not straightforward to calculate their van der Waals energy. However, in nonplanar geometries the potential between objects like slabs, cylinders, and spheres is still generally proportional to d^{-n}, with $n > 1$ (38). With Q_{II} interbilayer separations five or more times larger than the separation between bilayers in the L_α phase, the van der Waals attraction in the Q_{II} phase must be at least 5–10 times smaller than g_u of the L_α phase. To a good approximation, we can assume that all of g_u is expended in separating the bilayers to the distances within Q_{II} phases. The sum of the curvature and unbinding energy difference per lipid molecule between the Q_{II} and L_α phases, μ_Q, would then become

$$\mu_Q = \mu_Q^c + ag_u/2. \tag{14}$$

In Eq. 14, μ_Q^c is given by Eq. 10, a is the area per lipid molecule at the neutral planes of the monolayers, and the factor of 1/2 accounts for the presence of two monolayers per adhering bilayer.

In H_{II} phases of PEs and methylated PEs in excess water conditions, the interfacial separations, approximated as the H_{II} aqueous tube diameter, are typically 3.5–4 nm (23,26), ~2–3 times larger than the typical L_α interlamellar separation. This implies that the residual van der Waals attraction in the H_{II} phase is again significantly smaller than that in the L_α phase. We have not found expressions for van der Waals interactions in an H_{II} phase, but fortunately our argument concerning the relative effects of the unbinding energy g_u on T_Q and T_H turns out to be rather insensitive to the actual magnitude of the residual van der Waals term in the H_{II} phase. As an approximation, we assume that there is no residual interaction of the lipid monolayers in the H_{II} phase, similarly to our assumption for the Q_{II} phase. Then we can write an expression for the total energy difference between H_{II} and L_α per lipid molecule, μ_H, which is analogous to Eq. 14:

$$\mu_H = \mu_H^c + ag_u/2. \tag{15}$$

However, as shown below, the final result would be nearly the same even if we assumed that the van der Waals interaction energy per lipid molecule in the H_{II} phase has not changed and has remained equal to that of the L_α phase, so that Eq. 15 reduces to $\mu_H = \mu_H^c$.

Effects of the unbinding energy on T_Q and T_H

As is evident from Fig. 1 *A*, the curvature energy μ_Q^c initially decreases very slowly with increasing temperature, whereas the decline of μ_H^c is much steeper. If there is an additional positive free energy term besides the curvature energies that translates the free energy versus temperature curves upward, it is obvious that T_Q will increase by much more than T_H, because of the different slopes of μ_Q and μ_H. Below we consider the role of unbinding energy g_u, and Fig. 1, *B* and *C*, illustrates the effects on T_Q and T_H of g_u values typical of phospholipids.

In Fig. 1 *B*, μ_Q and μ_H are plotted using the same curvature energy parameters, but with $g_u = 0.01$ erg/cm^2. This is a relatively small value, typical for methylated PEs, PCs, and PC-cholesterol mixtures (Table 1). Relative to Fig. 1 *A*, where $g_u = 0$, T_Q increases by ~6 K to 56°C, whereas T_H increases by <0.3 K. T_H is still higher than T_Q, but the temperature range between L_α and H_{II} phases, where Q_{II} is the stable phase, has decreased from 12 K to only 6 K.

In Fig. 1 *C*, g_u is set at 0.15 erg/cm^2, which is typical of PEs in the L_α phase at room temperature (Table 1). Such a value results in a 25 K increase in T_Q to ~75°C, whereas T_H increases by only 4 K to 66°C. Notably, T_Q is now substantially higher than T_H and in such a system the H_{II} phase would form before the Q_{II} phase. Indeed, Fig. 1 *C* indicates that the Q_{II} phase would not become stable at any temperature. In summary, Fig. 1, *A–C*, shows that unbinding energies typically found in PEs can make $T_Q \geq T_H$. Elevating T_Q to above T_H effectively eliminates the Q_{II} phase from the sequence $L_\alpha \rightarrow Q_{II} \rightarrow H_{II}$ and reduces it to a direct $L_\alpha \rightarrow H_{II}$ phase transition. This effect explains the apparent absence of Q_{II} phases upon direct heating of PEs, whereas Q_{II} can be observed upon heating of monomethylated PEs (22) and PE mixtures with small amounts of PCs (39–42), which have much smaller values of g_u (Table 1). In some of these studies the presence of Q_{II} phases was inferred from observation of isotropic ^{31}P-NMR resonances and was not demonstrated by x-ray diffraction (39,40,42). However, the presence of isotropic ^{31}P-NMR resonances has been associated with Q_{II} phase formation in DOPE-Me (22,23,39), temperature-cycled DEPE (10,11) and DOPE (9,12), and soy PE/egg-PC (41).

A plot of T_Q and T_H as a function of g_u for a lipid with the elastic constants of DOPE-Me is shown in Fig. 2. T_Q increases much faster with g_u than T_H does and becomes greater than T_H for g_u values $>\sim$0.04 erg/cm^2. Since the effect of g_u on T_H is much smaller than that on T_Q, the results are not sensitive to the assumption in Eq. 15 regarding the g_u difference between the L_α and H_{II} phases. In the other limiting case, i.e., if we assume that g_u is the same in the L_α and H_{II} phases so that $\mu_H = \mu_H^c$, T_H would become independent of g_u, as indicated by the dotted line in Fig. 2. However, all conclusions of importance regarding the difference between T_Q and T_H as a functions of g_u would remain practically unaffected. The data in Table 1 and Fig. 2 suggest that addition of small amounts of PC to PE can reduce g_u to a level where there will be a direct $L_\alpha \rightarrow Q_{II}$ transition.

The g_u values in Table 1, which we used for the calculations shown in Fig. 1, *B* and *C*, have been determined at room temperature. They should be somewhat smaller at higher temperatures due primarily to an increase in the strength of repulsive undulation forces, since short-range hydration repulsion and van der Waals forces do not change appreciably with temperature (38,43). However, we are not aware of direct measurements of g_u in the temperature range above 40°C–50°C, where lamellar/nonlamellar phase transitions most often take place. A qualitative comparison of the unbinding energies of different lipids can sometimes be made on the basis of their lamellar spacings. For example, the lamellar spacing of DOPE-Me increases from 6.2 nm at 20°C to 6.4 nm at 65°C, whereas, in contrast, the lamellar spacing of DEPE decreases from 5.5 nm at 40°C to 5.2 nm at 60°C (44). Since the lamellar spacings in the methylated versus unmethylated PE are much larger at both low and high temperatures, and given the monotonic dependence of the attractive van der Waals forces between bilayers on interbilayer spacing, the unbinding energy of the PEs probably remains much larger than in methylated PE also at 60°C, similarly to the case at room temperature (Table 1). Thus, at least for temperatures up to 60°C, the temperature dependence of g_u should not affect our conclusions concerning the Q_{II} phase-forming propensities of these lipids.

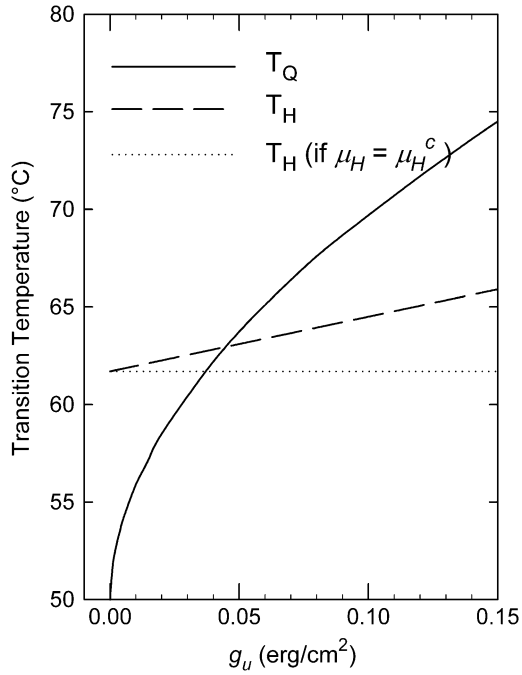

FIGURE 2 Dependence of the transition temperatures T_Q and T_H on the unbinding energy g_u for a lipid with the curvature elastic constants of DOPE-Me. The dashed horizontal line indicates the value of T_H if we assume that g_u in the H_{II} phase has remained equal to that of the L_α phase (see text).

DISCUSSION

Effect of unbinding energy on the inverted bicontinuous cubic phase stability

In this work we developed a simple argument that explains why dispersions of membrane lipids frequently display direct $L_\alpha \rightarrow H_{II}$ transitions, omitting the intermediate bicontinuous Q_{II} cubic phase. This argument makes use of the circumstance that the lipid L_α phase is stabilized relative to the Q_{II} phase by a noncurvature energy contribution, the unbinding energy g_u. Taking g_u into account shifts the temperature T_Q of the $L_\alpha \rightarrow Q_{II}$ transition upward. Our principal result, shown in Fig. 2, is that T_Q increases much faster with g_u and may readily become higher than the temperature T_H of a potential direct, higher temperature $L_\alpha \rightarrow H_{II}$ transition. Although an $L_\alpha \rightarrow Q_{II} \rightarrow H_{II}$ sequence of phases can be expected on theoretical grounds if one considers only the curvature energy differences between the lamellar and nonlamellar phases, at least for the range of PE elastic constants measured to date, we show that values of g_u that are typical of PEs with intermediate chain lengths of 16–18 carbon atoms are sufficiently large to prevent the Q_{II} phase from appearing as a stable phase between the L_α and H_{II} phases.

As can be seen in Fig. 2, for g_u values exceeding ~0.04 erg/cm^2, T_Q becomes greater than T_H, and Q_{II} becomes metastable with respect to the L_α and H_{II} phases. Such lipids would display direct $L_\alpha \rightarrow H_{II}$ transitions and eventually form some (trace) amount of metastable Q_{II} phase on cooling from the H_{II} range. Many PEs such as DEPE, DOPE, DPoPE, DPPE, and DHPE appear to conform to this type of phase behavior (Introduction). Moreover, dispersions of these lipids can be fully converted into Q_{II} phase by means of temperature cycling across the L_α/H_{II} phase transition. In all cases studied, amounts of Q_{II} phase that increase with increasing numbers of cycles were invariably found to form only during the cooling stage of the temperature cycles (11). On the other hand, it is known that short-chain PEs and glycolipids exhibit the sequences of phases $L_\alpha \rightarrow Q_{II} \rightarrow H_{II}$ (3,4,6,7). In the framework of this model, it may be that these lipids have smaller values of g_u than longer chain lipids and/

or a less negative value of M (Eqs. 9 and 10) that would allow a stable intermediate Q_{II} phase to form. It would be interesting to measure these quantities and see if this prediction is borne out.

However, lipids and lipid mixtures with values of g_u smaller than $\sim$0.04 erg/cm^2 (Table 1) and with appropriate spontaneous curvatures and bending elastic moduli would still be able to form intermediate Q_{II} phases upon heating. The best studied example of this kind, considered here in more detail, is DOPE-Me, whose behavior is consistent with the g_u value for *N*-monomethylated egg-PE (Table 1). Using the experimentally determined DOPE-Me elastic constants and substituting the latter g_u value in Eq. 14, one calculates an $L_\alpha \rightarrow Q_{II}$ transition temperature T_Q of 56°C. That is very close to the temperature of 55°C at which Q_{II} phase is first observed in DOPE-Me dispersions (22) (see also Fig. 3). Thus, the observed T_Q in DOPE-Me is consistent with the model for the Q_{II} curvature elastic energy in Eq. 10 and with the effect of g_u postulated in Eq. 14.

Fourth-order curvature energy expression for the Q_{II} phase

The reason for the use of higher order curvature terms in the expression for the Q_{II} phase curvature energy (Eq. 10) is treated in detail in the derivation of this model (15). If one uses only quadratic terms in the expression for the Q_{II} phase curvature energy, one obtains the unphysical result that the Q_{II} phase unit cell should contract indefinitely, which is incompatible with experiment (45). Obviously something stops that contraction of the unit cell size. For Q_{II} phases with very small lattice constants, one might expect that their contraction could be stopped by steric/hydration repulsion, but not for the PE Q_{II} phases considered here, which have lattice constants typically of more than 20 nm. Similarly to previous authors (e.g., Seddon and Templer (45) and Ljunggren and Eriksson (46)), we suggest that higher order curvature energy terms explain the stabilization of Q_{II} phases with large values of the equilibrium unit cell constant. The close correspondence noted above (within 1°) between observed and calculated values of T_Q indicates that the model developed in Siegel (15) is fairly accurate, at least in the temperature interval between T_K and T_Q. The Q_{II} phase is not the only system whose theoretical description requires a fourth-order curvature model. Such a model is also necessary to describe the prefission constriction of Golgi membrane tubules (47), for similar reasons.

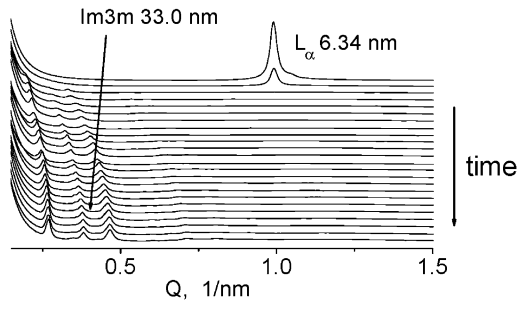

FIGURE 3 Direct transformation of the DOPE-Me lamellar L_α phase into bilayer cubic Im3m phase upon incubation at 55°C. The final Im3m lattice constant is 33.0 nm. Consecutive diffraction frames of 1 s exposure were recorded every 15 min. The sample was a 16.7% (w/v) DOPE-Me dispersion in PBS pH 7.2.

Mechanisms of inverted bicontinuous cubic phase formation

Our low-angle x-ray diffraction measurements show that Q_{II} phases can form by two different pathways in DOPE-Me dispersions (Figs. 3 and 4). These measurements were made at the Advanced Photon Source, Argonne, using a low-angle x-ray setup described in detail elsewhere (48). The first pathway is the direct $L_\alpha \rightarrow Q_{II}$ transition at constant temperature incubation (Fig. 3). It involves disordering (unbinding) of the L_α phase with concomitant formation of Q_{II} phase (Im3m under the conditions here). The lattice parameter of the Im3m phase gradually decreases with time and reaches a final value of 33.0 nm after 5–6 h of incubation. A slow disordering of the DOPE-Me L_α phase preceding the formation of the cubic phase in this lipid was also reported in previous work (23,49). Such a direct $L_\alpha \rightarrow Q_{II}$ transition may also take place at very slow rates of temperature increase (22).

If the incubation is long enough or the heating rate slow enough, one will observe Q_{II} phase formation at $T = T_Q$, and the value of g_u should strongly affect this value, as shown above (Fig. 2). The second pathway is indirect conversion in a heating-cooling cycle $L_\alpha \rightarrow H_{II} \rightarrow Q_{II}$ (Fig. 4). The heating rate of 1°C/min used in this cycle is obviously not slow enough to allow Q_{II} formation in the heating direction, and the dispersion first undergoes the $L_\alpha \rightarrow H_{II}$ transition.

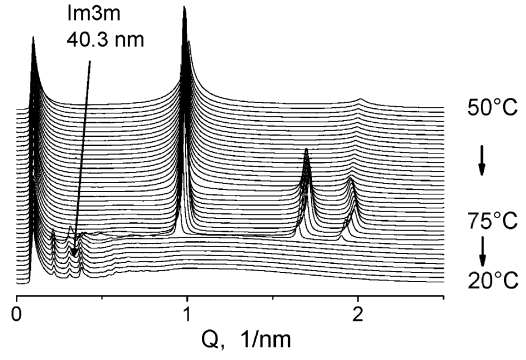

FIGURE 4 Complete conversion of the lamellar L_α phase into Im3m cubic phase in DOPE-Me dispersion in a single heating-cooling cycle $L_\alpha \rightarrow H_{II} \rightarrow$ Im3m. The Im3m lattice constant is 40.3 nm. Heating rate 1°C/min; cooling rate 5°C/min. Diffraction frames of 1 s exposure were recorded every 1 min. $L_\alpha \rightarrow H_{II}$ transition onset at 67.5°C. $H_{II} \rightarrow$ Im3m transition onset $\sim$55°C. The sample was a 10% (w/v) dispersion of DOPE-Me in PBS pH 7.2.

This is a clear indication for the existence of kinetic barriers that significantly slow down the formation of the Q_{II} phase even though it is the thermodynamically stable phase in the respective temperature range. On the other hand, an $H_{II} \rightarrow Q_{II}$ transition in cooling turns out to be very fast, 1–2 orders of magnitude faster than the $L_\alpha \rightarrow Q_{II}$ transition, and the DOPE-Me dispersion fully converts into Q_{II} phase (Im3m phase with lattice parameter of ~40 nm in Fig. 4) without any traces of reappearing L_α phase.

Cubic phase formation in PEs

Although DOPE-Me readily forms Q_{II} phase in a single heating-cooling cycle, this is not the case for PE dispersions, which typically require several tens of cycles for complete conversion into the Q_{II} phase (11). We speculate that only a fraction of the lipid in the H_{II} phase enters the Q_{II} phase on each cooling cycle in PEs because the unbinding energy g_u is ~15 times larger for PEs than for monomethylated PEs (Table 1). This would strongly favor recovery of the L_α phase on cooling from the H_{II} range at the expense of Q_{II} formation. However, the Q_{II} fraction, once it forms, is stable upon supercooling into the L_α phase region, even down to the chain-melting temperature of the dispersion (9,11), so Q_{II} phase accumulates during successive cycles until it completely replaces the L_α phase.

In earlier work we found that salts (NaSCN, NaCl, NaH_2PO_4, Na_2SO_4) as well as sugars (sucrose, trehalose) substantially reduced the number of cycles necessary to convert PE dispersions into the Q_{II} phase (11). The relative efficacy of the Na salts in promoting Q_{II} phase formation did not appear to correlate with salt ordering in the lyotropic series. The data, rather, appeared to indicate that the accelerating solutes destabilize to some extent the L_α phase and maintain some portion of the sample in a state of uncorrelated, single bilayers. We considered these disordered bilayers a more likely source for formation of cubic phases on the grounds elaborated in this work, i.e., that the attractive interactions in a well-stacked lamellar phase, which could be expected to impede the formation of a bicontinuous cubic phase, would be much weaker between bilayers separated by larger spaces (11). Recently it has been shown that monovalent salts and small carbohydrate molecules decrease the van der Waals attraction between electrostatically neutral bilayers in the L_α phase (50,51). Therefore, it appears that these solutes are effective in accelerating Q_{II} phase formation because they decrease the unbinding energy g_u and thus facilitate the bilayer separation.

Physiological relevance

Because of the effect of g_u, for lipid bilayers with elastic constants such that $T_K < T_H$ and with $g_u > 0$, there is a range of temperatures in which the Q_{II} phase is metastable with respect to the L_α phase, but represents the stable configuration with respect to unbound, disordered bilayers for which $g_u = 0$. Consider two bilayers composed of lipid which is in this temperature range of metastable Q_{II} phase under the ambient conditions. The bilayers are maintained in the unbound state by some external factor, such as the presence of hydrated macromolecules between them. If the two bilayer interfaces are opposed over a small area, the lipids in this region might then be able to spontaneously form structures like fusion pores, which may be considered Q_{II} phase precursors (14,15). In these cases where unbinding factors are present, lipid compositions might be more fusogenic than indicated by their bulk phase behavior in the absence of such factors.

PCs are examples of membrane lipids that are effective in reducing g_u (Table 1). In model systems, lipid molecules with bulky headgroups such as polyethylene glycol (PEG)-conjugated phospholipids can be particularly effective in this. In previous work we have shown that 5 mol % of PEG-conjugated dimyristoyl PE (DMPE-PEG510) disorders the L_α phase and promotes formation of stable intermediate Q_{II} phase in a temperature range between the L_α and H_{II} phases in DEPE dispersions (44,52). Even at low concentrations, the PEG lipids appear to create steric hindrances that prevent the bilayer stacking into L_α phase and thus favor formation of Q_{II} phases.

Protocols for measuring the Gaussian (saddle splay) curvature elastic modulus

The big effect of the unbinding energy g_u on the temperature T_Q of the L_α/Q_{II} transition has important implications for the choice of protocols for measuring the Gaussian curvature elastic modulus κ of membranes. Recently two such protocols were suggested based on observations of Q_{II} phase behavior (14,15). The method in Siegel and Kozlov (14) relies on a measurement of T_Q. The method in Siegel (15) is based on measurements of the Q_{II} phase unit cell constant as a function of temperature. The results of the latter protocol do not depend on the value of T_Q and, since T_Q is strongly affected by g_u, it is clear that the utility of the technique in Siegel and Kozlov (14) is more limited than the technique in Siegel (15). The techniques in Siegel and Kozlov (14) and Siegel (15) will yield measurements of similar accuracy limited by the accuracy of values of δ, k_m, J_s, and their temperature dependences. However, for comparative measurements on a host lipid system with minor fractions of lipid or peptide additives, the precision of comparisons by the technique in Siegel (15) will be superior because of the lack of a g_u effect. This is significant for studies of the mechanism of membrane fusion and fission because the Gaussian curvature modulus has almost as large an effect on the curvature energy of the stalk fusion intermediate as the monolayer bending modulus (16). It would be important to measure the effects of lipid composition and of moieties of fusion- or fission-catalyzing proteins on this modulus.

Use of the advanced photon source was supported by the U.S. Department of Energy under contract No. W-31-102-Eng-38. DuPont-Northwestern-Dow Collaborative Access Team is supported by E. I. DuPont de Nemours, Dow Chemical, the National Science Foundation through grant DMR-9304725, and the state of Illinois through the Department of Commerce and the Board of Higher Education grant IBHE HECA NWU 96. BioCAT is a National Institutes of Health (NIH)-supported research center through grant RR08630. B.G.T. acknowledges support from NIH grant GM57305 and from the Center for Cancer Nanotechnology Excellence initiative of the NIH National Cancer Institute under award U54CA119341.

REFERENCES

1. Seddon, J. M., and R. H. Templer. 1995. Polymorphism of lipid-water systems. *In* Handbook of Biological Physics. R. Lipowsky and E. Sackmann, editors. Elsevier Science, Amsterdam. 97–160.
2. Lewis, R. N. A. H., D. A. Mannock, and R. N. McElhaney. 1997. Membrane lipid molecular structure and polymorphism. *In* Lipid Polymorphism and Membrane Properties (Current Topics in Membranes, Vol. 44). R. Epand, editor. Academic Press, San Diego, CA. 25–102.
3. Seddon, J. M., G. Cevc, R. D. Kaye, and D. Marsh. 1984. X-ray-diffraction study of the polymorphism of hydrated diacylphosphatidylethanolamine and dialkylphosphatidylethanolamine. *Biochemistry.* 23:2634–2644.
4. Hinz, H. J., H. Kuttenreich, R. Meyer, M. Renner, R. Frund, R. Koynova, A. I. Boyanov, and B. G. Tenchov. 1991. Stereochemistry and size of sugar head groups determine structure and phase-behavior of glycolipid membranes—densitometric, calorimetric, and x-ray studies. *Biochemistry.* 30:5125–5138.
5. Koynova, R., and R. C. MacDonald. 2007. Natural lipid extracts and biomembrane-mimicking lipid compositions are disposed to form non-lamellar phases, and they release DNA from lipoplexes most efficiently. *Biochim. Biophys. Acta.* 1768:2373–2382.
6. Koynova, R., and M. Caffrey. 1994. Phases and phase-transitions of the hydrated phosphatidylethanolamines. *Chem. Phys. Lipids.* 69:1–34.
7. Koynova, R., and M. Caffrey. 1994. Phases and phase-transitions of the glycoglycerolipids. *Chem. Phys. Lipids.* 69:181–207.
8. Koynova, R., B. Tenchov, and G. Rapp. 1997. Mixing behavior of saturated short-chain phosphatidylcholines and fatty acids—eutectic points, liquid and solid phase immiscibility, non-lamellar phases. *Chem. Phys. Lipids.* 88:45–61.
9. Shyamsunder, E., S. M. Gruner, M. W. Tate, D. C. Turner, P. T. C. So, and C. P. S. Tilcock. 1988. Observation of inverted cubic phase in hydrated dioleoylphosphatidylethanolamine membranes. *Biochemistry.* 27:2332–2336.
10. Veiro, J. A., R. G. Khalifah, and E. S. Rowe. 1990. P-31 nuclear-magnetic-resonance studies of the appearance of an isotropic component in dielaidoylphosphatidylethanolamine. *Biophys. J.* 57:637–641.
11. Tenchov, B., R. Koynova, and G. Rapp. 1998. Accelerated formation of cubic phases in phosphatidylethanolamine dispersions. *Biophys. J.* 75:853–866.
12. Erbes, J., C. Czeslik, W. Hahn, R. Winter, M. Rappolt, and G. Rapp. 1994. On the existence of bicontinuous cubic phases in dioleoylphosphatidylethanolamine. *Ber. Bunsenges. Phys. Chem.* 98:1287–1293.
13. Jordanova, A., Z. Lalchev, and B. Tenchov. 2003. Formation of monolayers and bilayer foam films from lamellar, inverted hexagonal and cubic lipid phases. *Eur Biophys J.* 31:626–632.
14. Siegel, D. P., and M. M. Kozlov. 2004. The Gaussian curvature elastic modulus of *N*-monomethylated dioleoylphosphatidylethanolamine: relevance to membrane fusion and lipid phase behavior. *Biophys. J.* 87: 366–374.
15. Siegel, D. P. 2006. Determining the ratio of the Gaussian curvature and bending elastic moduli of phospholipids from Q(II) phase unit cell dimensions. *Biophys. J.* 91:608–618.
16. Kozlovsky, Y., A. Efrat, D. A. Siegel, and M. M. Kozlov. 2004. Stalk phase formation: effects of dehydration and saddle splay modulus. *Biophys. J.* 87:2508–2521.
17. Helfrich, W. 1973. Elastic properties of lipid bilayers—theory and possible experiments. *Z Naturforsch [C]* 28:693–703.
18. Mitov, M. D. 1978. 3rd and 4th order curvature elasticity of lipid bilayers. *Comptes Rendus de l'Academie Bulgare des Sciences.* 31: 513–515.
19. do Carmo, M. P. 1976. Differential Geometry of Curves and Surfaces. Prentice-Hall, Englewood Cliffs, NJ. 212.
20. Anderson, D. M., S. M. Gruner, and S. Leibler. 1988. Geometrical aspects of the frustration in the cubic phases of lyotropic liquid-crystals. *Proc. Natl. Acad. Sci. USA.* 85:5364–5368.
21. Schwarz, U. S., and G. Gompper. 2001. Bending frustration of lipid-water mesophases based on cubic minimal surfaces. *Langmuir.* 17:2084–2096.
22. Cherezov, V., D. P. Siegel, W. Shaw, S. W. Burgess, and M. Caffrey. 2003. The kinetics of non-lamellar phase formation in DOPE-Me: relevance to biomembrane fusion. *J. Membr. Biol.* 195:165–182.
23. Gruner, S. M., M. W. Tate, G. L. Kirk, P. T. C. So, D. C. Turner, D. T. Keane, C. P. S. Tilcock, and P. R. Cullis. 1988. X-ray-diffraction study of the polymorphic behavior of *N*-methylated dioleoylphosphatidylethanolamine. *Biochemistry.* 27:2853–2866.
24. Tate, M. W., and S. M. Gruner. 1989. Temperature-dependence of the structural dimensions of the inverted hexagonal (HII) phase of phosphatidylethanolamine-containing membranes. *Biochemistry.* 28: 4245–4253.
25. Fuller, N., and R. P. Rand. 2001. The influence of lysolipids on the spontaneous curvature and bending elasticity of phospholipid membranes. *Biophys. J.* 81:243–254.
26. Harper, P. E., D. A. Mannock, R. N. A. H. Lewis, R. N. McElhaney, and S. M. Gruner. 2001. X-ray diffraction structures of some phosphatidylethanolamine lamellar and inverted hexagonal phases. *Biophys. J.* 81:2693–2706.
27. Lewis, R. N. A. H., D. A. Mannock, R. N. McElhaney, D. C. Turner, and S. M. Gruner. 1989. Effect of fatty acyl chain-length and structure on the lamellar gel to liquid-crystalline and lamellar to reversed hexagonal phase-transitions of aqueous phosphatidylethanolamine dispersions. *Biochemistry.* 28:541–548.
28. Epand, R. M., N. Fuller, and R. P. Rand. 1996. Role of the position of unsaturation on the phase behavior and intrinsic curvature of phosphatidylethanolamines. *Biophys. J.* 71:1806–1810.
29. Templer, R. H., B. J. Khoo, and J. M. Seddon. 1998. Gaussian curvature modulus of an amphiphilic monolayer. *Langmuir.* 14:7427–7434.
30. Nagle, J. F., and S. Tristram-Nagle. 2000. Structure of lipid bilayers. *Biochim. Biophys. Acta* 1469:159–195.
31. McIntosh, T. J., and S. A. Simon. 1996. Adhesion between phosphatidylethanolamine bilayers. *Langmuir.* 12:1622–1630.
32. Rand, R. P., and V. A. Parsegian. 1989. Hydration forces between phospholipid-bilayers. *Biochim. Biophys. Acta.* 988:351–376.
33. Needham, D. 1993. Measurement of interbilayer adhesion energies. *Methods Enzymol.* 220:111–129.
34. Needham, D., and D. V. Zhelev. 2000. Use of micropipette manipulation techniques to measure the properties of giant lipid vesicles. *In* Giant Vesicles. P. L. Luisi and P. Walde, editors. John Wiley & Sons, New York. 103–147.
35. Evans, E., and D. Needham. 1987. Physical properties of surfactant bilayer-membranes—thermal transitions, elasticity, rigidity, cohesion, and colloidal interactions. *J. Phys. Chem.* 91:4219–4228.
36. Evans, E., and D. Needham. 1986. Giant vesicle bilayers composed of mixtures of lipids, cholesterol and polypeptides—thermomechanical and (mutual) adherence properties. *Faraday Discuss. Chem. Soc.* 81: 267–280.
37. Kraineva, J., R. A. Narayanan, E. Kondrashkina, P. Thiyagarajan, and R. Winter. 2005. Kinetics of lamellar-to-cubic and intercubic phase

transitions of pure and cytochrome *c* containing monoolein dispersions monitored by time-resolved small-angle x-ray diffraction. *Langmuir*. 21:3559–3571.

38. Parsegian, V. A. 2006. Van der Waals Forces. Cambridge University Press, Cambridge, UK.
39. Ellens, H., D. P. Siegel, D. Alford, P. L. Yeagle, L. Boni, L. J. Lis, P. J. Quinn, and J. Bentz. 1989. Membrane-fusion and inverted phases. *Biochemistry*. 28:3692–3703.
40. Tilcock, C. P. S., M. B. Bally, S. B. Farren, and P. R. Cullis. 1982. Influence of cholesterol on the structural preferences of dioleoylphosphatidylethanolamine dioleoylphosphatidylcholine systems—A P-31 and deuterium nuclear magnetic-resonance study. *Biochemistry*. 21: 4596–4601.
41. Tilcock, C. P. S., P. R. Cullis, and S. M. Gruner. 1986. On the validity of P-31-NMR determinations of phospholipid polymorphic phase-behavior. *Chem. Phys. Lipids*. 40:47–56.
42. Separovic, F., and K. Gawrisch. 1996. Effect of unsaturation on the chain order of phosphatidylcholines in a dioleoylphosphatidylethanolamine matrix. *Biophys. J*. 71:274–282.
43. Simon, S. A., S. Advani, and T. J. McIntosh. 1995. Temperature-dependence of the repulsive pressure between phosphatidylcholine bilayers. *Biophys. J*. 69:1473–1483.
44. Koynova, R., B. Tenchov, and G. Rapp. 1997. Low amounts of PEG-lipid induce cubic phase in phosphatidylethanolamine dispersions. *Biochim. Biophys. Acta*. 1326:167–170.
45. Seddon, J. M., and R. H. Templer. 1993. Cubic phases of self-assembled amphiphilic aggregates. *Philos. Trans. R. Soc. Lond. A*. 344:377–401.
46. Ljunggren, S., and J. C. Eriksson. 1992. Minimal-surfaces and Winsor III microemulsions. *Langmuir*. 8:1300–1306.
47. Shemesh, T., A. Luini, V. Malhotra, K. N. J. Burger, and M. M. Kozlov. 2003. Prefission constriction of Golgi tubular carriers driven by local lipid metabolism: a theoretical model. *Biophys. J*. 85:3813–3827.
48. Tenchov, B. G., R. C. MacDonald, and D. P. Siegel. 2006. Cubic phases in phosphatidylcholine-cholesterol mixtures: cholesterol as membrane ''fusogen''. *Biophys. J*. 91:2508–2516.
49. Siegel, D. P., and J. L. Banschbach. 1990. Lamellar/inverted cubic (L alpha/QII) phase transition in *N*-methylated dioleoylphosphatidylethanolamine. *Biochemistry*. 29:5975–5981.
50. Deme, B., M. Dubois, and T. Zemb. 2002. Swelling of a lecithin lamellar phase induced by small carbohydrate solutes. *Biophys. J*. 82: 215–225.
51. Petrache, H. I., S. Tristram-Nagle, D. Harries, N. Kucerka, J. F. Nagle, and V. A. Parsegian. 2006. Swelling of phospholipids by monovalent salt. *J. Lipid Res*. 47:302–309.
52. Koynova, R., B. Tenchov, and G. Rapp. 1999. Effect of PEG-lipid conjugates on the phase behavior of phosphatidylethanolamine dispersions. *Colloids Surf. A Physicochem. Eng. Aspect*. 149:571–575.